ILASS 2008
Sep. 8-10, 2008, Como Lake, Italy

Paper ID ILASS08-7-7

DROP SIZE MEASUREMENT TECHNIQUES APPLIED TO GASOLINE SPRAYS

Nicolas Fdida*, Jean-Bernard Blaisot°, Alain Floch[$], David Dechaume[+]

*CORIA CNRS-UMR 6614, nicolas.fdida@coria.fr
° CORIA CNRS-UMR 6614, jean-bernard.blaisot@coria.fr
[$]Renault SAS, alain.floch@renault.com
[+]Renault SAS, david.dechaume@renault.com

ABSTRACT
Combustion processes involved in internal combustion engines greatly depend on the characteristics of the spray. This study is focused on the comparison of three different techniques used for spray drop sizing. Laser diffraction (LDG), phase Doppler anemometry (PDA) and Image Analysis (IMA) have been used to characterize gasoline sprays produced by gasoline injectors of a direct injection type. Whereas studies comparing drop sizing techniques found in the literature are mainly dealing with steady flows, attention is paid here to the unsteady nature of the spray. The differences in the measurement volumes of the different techniques are also considered. As these diagnostics do not measure exactly the same kind of distribution, both PDA and IMA measurements were converted to spatial-averaged volume-weighted drop size distributions to be compared to LDG. The Sauter Mean Diameter D_{32} and the mean diameter D_{43} are used to characterize the spray for different time and position of the measurement volume in the spray. The comparison between the three techniques shows a good agreement. Greatest mean diameters are found on the leading edge of the spray and on the side of the spray facing stagnant air, so where the conditions are favourable to a fast evaporation of the smallest droplets. Velocity measurements done by PDA and drop shape morphology characterization are also discussed.

1. INTRODUCTION

The combustion process of internal combustion engines greatly depends on the atomization, the spreading and the vaporization of the fuel and on the mixing in the combustion chamber. The key parameter that determines many aspects of this cascade phenomenon is the drop size distribution of the spray.

This feature of the spray is an input parameter for combustion computations and its reliability controls the relevance of the computation results. This parameter can be directly introduced in combustion codes or obtained from a computation code for atomization. Whatever the case, calibration has to be done through comparison with experimental results.

The drop size distribution is a relatively complex property of the spray and need to be reduced to a finite number of parameters. The Sauter Mean Diameter (D_{32}) and the mean diameter of the volume-weighted distribution (D_{43}) are common parameters used to qualify a spray and are used here to compare drop size measurements. Measurement features like the measurement volume has to be clearly defined in order to be correctly implemented in computation codes. Moreover, for non-stationary sprays, the time resolution has to be well defined also. Additional parameters like drop velocity and drop shape can also be relevant in some cases.

Drop size distributions are measured with a laser diffraction granulometer (LDG), a shadow Imaging Technique (IMA) and a phase Doppler anemometer (PDA). Measurements are made on a gasoline spray produced by a direct injection system. Due to the unsteady nature of the spray, the evolution of mean diameters and of the drop size distributions was considered. This could be obtained thanks to the time-resolved measurement of PDA and to the high acquisition rate of LDG (2.5kHz). Regarding IMA technique, as the frame rate does not allow to perform time-resolved acquisition, snapshots of the spray were recorded at different times to cover the injection duration.

The drop size distribution is characterized at two downstream locations in the spray but without doing a complete mapping in each cross section. The measurement volumes and the measurement periods are different for the three techniques. Indeed PDA gives a time-resolved characterization of the droplets passing at a given point in the flow whereas LDG and IMA give a snapshot of the spray at a given time and over a given volume. However a particular attention has been paid to make comparable the data given by PDA to those provided by LDG and IMA. This was performed thanks to the velocity measured with PDA.

As aim of this study is to control the ability of the three techniques to give useful data for CFD codes, the focus has been put on how to perform the most relevant characterization of the spray with as few measurement as possible. Whereas the spray is not axi-symmetric, the deconvolution of LDG data is thus not considered to limit the number of measurement points.

2. EXPERIMENTAL SETUP

2.1 Test bench

The injector is a six-hole commercial high-pressure injector used for direct injection engine. The arrangement of the holes is shown in Figure 1. Only the spray produced by one of the six holes is considered here (i.e. the jet number 3 on Fig. 1). Isooctane (2,2,4 trimethylpentane) is used as fuel, the injection duration is fixed to 3 ms and the injection pressure is

set to 10 MPa. Back pressure remains in atmosphere conditions for all the experiments.

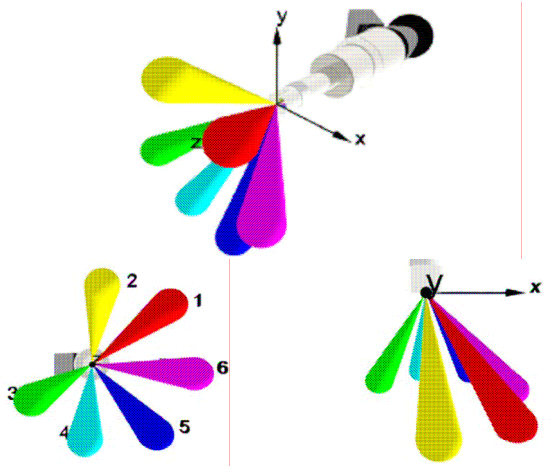

Figure 1 Scheme of the spray of the injector

The injector is oriented in such a way that the studied jet is sprayed vertically as shown on Figure 2. Measurement locations @ z=30 mm are represented by circles in dot lines in this figure. The spray is characterized at two downstream locations from the nozzle exit (z=30 mm and z=60 mm). Six time periods have been considered during the injection duration to study the time dependence of the characteristics of the spray. These periods are indicated in Table 1 and were chosen in order to represent the different phases of the behaviour of the spray. The time evolution of the transmission of light *T*, given by LDG, was considered to do this. At the beginning of the injection, the transmission decreases during 1.2 ms. The periods T1 and T2 belong to this phase. A stationary phase follows (~3 ms, periods T3 and T4) and for the last phase (periods T5 and T6) the transmission increases until there is no longer any drop in the laser beam of LDG. The duration of the six periods is the same and is equal to the inverse of the acquisition rate of LDG, i.e. 0.4 ms.

Some particular phenomena have been observed on the spray produced by the six orifices that cannot be seen on the overall view of the spray in Figure 2. Indeed, the jets 2 and 3 are more sensitive to high aerodynamic interaction with ambient air because they are not surrounded by other jets like the jets 1 and 4 to 6. At the beginning of the injection, cycle-to-cycle fluctuations of the head position of the jet 3 have been observed. This is probably due to either high velocity gradients between the spray and the ambient air or fluctuations of the hydraulic delay. Moreover during the stationary phase of the flow, drop concentration variations in the spray show the same kind of cycle-to-cycle fluctuation. This has been confirmed in reduced field visualizations. Indeed for a given time and position, image series present high fluctuations of the droplet density.

Time periods *Tn*	z = 30mm	z = 60mm
T1	0.0 – 0.4 ms	0.4 – 0.8 ms
T2	0.4 – 0.8 ms	0.8 – 1.2 ms
T3	1.2 – 1.6 ms	1.6 – 2.0 ms
T4	2.4 – 2.8 ms	2.8 – 3.0 ms
T5	3.2 – 3.6 ms	3.6 – 4.0 ms
T6	4.0 – 4.4 ms	4.4 – 4.8 ms

Table 1 Reference time periods defined from LDG measurements

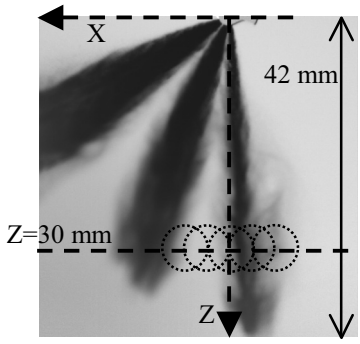

Figure 2 Locations of the measurement positions in the spray

2.2 Laser diffraction granulometer (LDG)

The laser diffraction granulometer (LDG) used to characterize the spray is a *Malvern-Insitec Spraytec* model with a laser diode ($\lambda = 670$ nm). The laser beam is 6 mm in diameter. A receiving lens of focal length 100 mm was used to measure particle sizes from 1.9 µm to 200 µm. The drop size range of LDG is thus well suited to this gasoline spray. Moreover, the measurement rate is fixed to its maximum value (2 500 measurements/sec). This allows to obtain a time-resolved characterization of the spray over the injection duration. Due to the high density of the spray, the attenuation A ($A = 100 - T$) of the laser beam for these experiments was often above the 60 %. In such conditions, Triballier et al. [1] showed that a multiple-scattering correction had to be performed. The correction proposed by the commercial software controlling the apparatus was thus switched on for all experiments.

2.3 Phase Doppler Anemometry (PDA)

A commercial *Dantec PDPA* system has been used for PDA testing. An Argon laser delivers green ($\lambda_g = 514.5$ nm) and blue ($\lambda_b = 488$ nm) beams. The beam separation in the transmitting head is 40 mm and the focal length of the lens is $f_t = 250$ mm. The focal length of the receiver lens is $f_r = 160$ mm.

The *Fiber Flow* mode was selected with this commercial PDA. With this mode, the curvature of each drop is measured in only one direction. The *Fiber Flow* mode was used for its high data rate and its relatively easy setup.

The off-axis angle of the receiving assembly was set to $\phi = 77°$ in the forward direction. This setting corresponds to the Brewster angle for isooctane ($n = 1.392$) and is used to decrease the effect of trajectory ambiguity arising when both reflected and refracted light are collected by the receiving optics [2,3]. The maximum diameter is $D_{max} = 62$ µm in this configuration. For each measurement location, a maximum number of 200 000 droplets is fixed to end the measurement. Then, data are sorted in order to count the droplets passing through the measurement volume during each time period Tn of 0.4 ms. As the injection duration is 3 ms, the resulting average number of droplets counted for each position and time period can be very low. It ranges from 5 000 to 20 000 droplets depending on the time and location of the measurement. Moreover, only the droplets satisfying a spherical validation criterion are counted in the final drop-size. It eliminates droplets presenting a difference higher than

25% between the diameters measured by two different detectors placed in the same plane.

2.4 Shadow Imaging Technique (IMA)

The spray is illuminated in a backlight configuration by a non-coherent short flash source (Nanotwin-HSPS, duration ~ 12ns) to freeze the droplets on the images. The detector of the monochrome camera is composed of 1 200 x 1 600 square pixels of 7.4 µm side. A long working distance microscope (Isooptic) of lateral magnification $\gamma = 10.5$ is used to obtain high-resolution images. The field of view is 1.12 mm x 0.85 mm and the resolution is 1 419 pixels/mm. The average number of droplets counted for each measurement position ranges from 5 000 to 10 000 droplets depending on the time and location of the measurement.

A 3-step homemade image-processing program developed in C++ is applied to images. The first step consists of a normalization of the images to enhance the contrast of the images and to correct non-uniform background illumination. In a second step, images are binarized using two thresholding techniques. A classical threshold based on the range of grey-level in the image and a threshold based on the wavelet transform (in order to detect the out-of-focus droplets). This technique allows detection of local grey level variations of low contrast images in order to localize the maximum number of droplets and to associate to each of them a surrounding mask.

Then each droplet is separated from its neighbours within the mask in order to be individually analyzed. The sub-pixel contour of the droplet is computed. The diameter of each droplet is defined as the equivalent surface diameter of the binarized image of the droplet at a level equal to 61% of the local grey level amplitude. A calibration procedure is achieved to estimate correctly the diameter [4]. The calibration procedure consists in taking images of calibrated discs engraved on a glass substrate for several distances from the focus plane of the camera. The ratio of the real diameter to the computed value is directly related to the contrast of the droplets, as shown on Figure 3. Thus a regression curve is computed to estimate the real diameter of the drops.

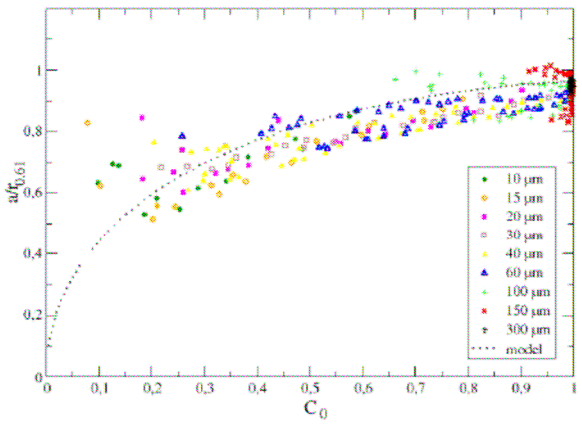

Figure 3: Calibration of sizing procedure with calibrated discs from 10 to 300 µm [4].

The level of out-of-focus of each droplet is determined in order to sort the droplets relatively to their spatial position from the focus plane. This is achieved through the calibration of the Point Spread Function (*PSF*) of the optical setup (See Figure 4). Indeed, the *PSF* gives information on the out-of-focus of droplets [4]. Droplets of low contrast (< 0.1) and of high level of out-of-focus (*PSF* >0.02 mm) are so rejected.

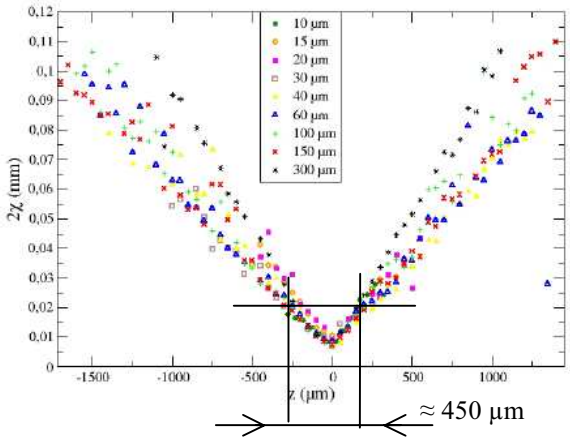

Figure 4: Calibration of the *PSF* with calibrated discs from 10 to 300 µm [4].

Moreover, as PDA measurements take into account the droplets sphericity, we eliminate the non-spherical droplets (sphericity *Sp*>0.4, see section 3.4). Indeed, the injector produces rather small droplets (D < 50 µm) that are essentially spherical. However non-spherical droplets and ligaments were detected with IMA until the time period T3 @ z = 30mm, as we can see on Figure 5.

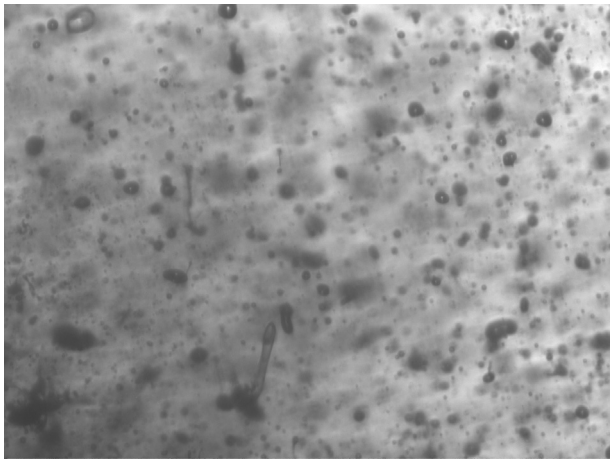

Figure 5: Example of image @ z = 30mm, x =0, T4

2.5 Measurement volume and temporal coincidence

To compare the measurement techniques and to characterize the spray at the same points, the size of the measurement volume V_m has to be evaluated for each technique. For LDG, V_m^{LDG} results from the intersection between the spray and the laser beam. This volume is a cylinder of 6 mm in diameter but is not fixed in length a priori. The length of this cylinder along y axis is about 10 mm and 20 mm respectively for the 2 downstream positions z = 30mm and z = 60mm.

For PDA the measurement volume V_m^{PDA} results from the intersection of the laser beams, producing a cigar shape that is 933 µm long and 75 µm in diameter. V_m^{PDA} is thus 0.005 mm^3 and is 60 000 times smaller than V_m^{LDG}. Moreover, droplets of different sizes can be detected through different detection

volumes. Indeed, as the laser beam has a Gaussian intensity distribution, a small drop passing near the edge of V_m^{PDA} may not be detected whereas a big one will be. This can lead to an underestimation of the population of the smallest drops *[5]*. This bias can be corrected by a procedure called PVC (Probe Volume Correction) that determines the effective detection area for each category of droplet size. In our case no correction was applied as no correlation had been found between drop size and the effective detection volume.

For IMA, the measurement volume V_m^{IMA} is defined by the image field (1.12 mm x 0.85 mm) and the depth of field, estimated via the criterion on the *PSF* width. A maximum *PSF* width of 20 µm corresponds to a depth of field of ≈ 450 µm [4] (see Figure 4). It results in a measurement volume $V_m^{IMA} \approx 0.4$ mm^3. This criterion was chosen according to the limit of visibility of the smallest detectable drops (D<5 µm) in the spray.

Measurement volumes of LDG and PDA are both roughly cylindrical with their main axis oriented perpendicularly to the *z* axis, so perpendicularly to the main direction of the flow. But V_m^{PDA} is around 60 000 times smaller than V_m^{LDG}. The measurement volume of IMA is a parallelepiped with a very thin depth along the *y* axis. As measurement volumes are not the same, especially the lateral sizes, attention must be focused on the droplets sampled by each technique. The droplets enter the measurement volume of LDG before to enter the one of PDA. To take this into account, a time shift of around 0.06 ms (based the mean velocity of the spray) has been applied between measurement periods for LDG and PDA. As the lateral sizes of V_m^{IMA} is about 1 mm, the time spent by the drops to reach V_m^{PDA} is only ~ 40 µs, thus no time shift was applied for IMA.

Ideally, if the measurement volume of each technique is placed at the same location, the time for the first detected droplets in V_m would be the same for the three techniques. For PDA, the first droplets were detected between 0.6 and 0.7 ms. For IMA, the first droplets coming into the images are recorded at 0.7 ms. For LDG, the first validated measurement (i.e. with a sufficient attenuation) is recorded during the period time [0;0.4] ms. The spray is probably entering V_m^{LDG} during this time period, but it was hard to check because the real time recording sequence of LDG is not known. Only few droplets, those moving faster than 70 m/s, could enter V_m^{LDG} within this time period of 0.4 ms at the downstream position *z* = 30 mm.

2.6 Comparison of probability density functions

LDG gives a result proportional to the spatial frequency of the drops, referred to as a spatial average, as for IMA. On the other hand, PDA measures the number of drops per unit time passing through the sample volume. Therefore, the PDA measures a temporal average. Dodge and al. [6] clearly explain that if droplet size and velocity are not correlated, the temporal and spatial averages are identical. However, in many spray systems the velocities are correlated with size, almost due to the variations in drag with diameter. The temporal and spatial averages are thus different. The conversion from temporal-averaged to spatial-averaged data can be performed by dividing the probability density function (*pdf*) of a temporal average by the mean velocity for each diameter class in the average summation. Thus, the PDA size distributions have been expressed as spatial averages for comparison with the LDG and IMA results.

Moreover, LDG measures size distributions by volume (f_v) whereas PDA and IMA measure size distributions by number (f_n) as they are actually based on a counting of the droplets. The distributions measured with PDA or IMA have been converted to volume fractions by using the well known relation between distributions by volume and distributions by number:

$$f_v = \frac{f_n(D).D^3}{D_{30}^3} \qquad (1)$$

3. RESULTS

3.1 Mean drop size diameter

The comparison of the mean diameters D_{32} and D_{43} measured at *z* = 30 mm are given in Figure 6 (LDG (square), PDA (triangle) and IMA (circle)). The filled markers are related to D_{32} and the empty markers are associated to D_{43}. Whereas measurement volumes are really different, we can see that trends and values are in a relatively good agreement between the three drop-sizing techniques for either D_{32} and D_{43}. PDA and LDG are in a good agreement for the positions *x*=0 and *x*=+/- 3 mm, that are in the dense zone of the spray. On the edge of the spray, LDG gives the highest values for *x*=+ 6 mm, i.e. the side where the jet interacts with the others. The size of V_m^{LDG} is very large, 6 mm in diameter, compared to V_m^{PDA}. As we can see on Figure 2, some droplets coming from the side of the jet probably pass through the laser beam of LDG for this position. Despite this difference, we can say that the mean diameter values are in a good agreement between the three techniques. On the other side *x*=- 6 mm, where the jet is directly facing the ambient air, IMA and LDG are in a good agreement concerning the time evolution but PDA gives a different trend. PDA gives the highest values for this position *x*=- 6 mm. It is probably due to the fact that very few droplets pass through V_m^{PDA} for this position and the data rate is very low (<100 particles/s) whereas on the other side, this rate is much greater (>500 particles/s).

D_{32} and D_{43} measured by IMA are lower by one to two microns than the values measured by LDG and PDA. This could be explained by the difference between the V_m. Indeed, V_m^{IMA} is thinner along *y* axis (~ 0.45 mm for IMA, ~ 0.9 mm for PDA and ~ 10 mm for LDG). Additional droplets taken into account in V_m^{PDA} or V_m^{LDG} and not in V_m^{IMA} are those who are placed on the edge of the spray. The criterion on the PSF has an influence on the mean diameters values. Indeed, the increase of the maximum PSF value from 10 to 30 µm induces higher values for mean diameters. It means that the extension of V_m^{IMA} along y axis increases the counting of big droplets (D > 20µm). This phenomenon is due to the better visibility of the biggest droplets in IMA technique and the presence of bigger drops on the edge of the spray.

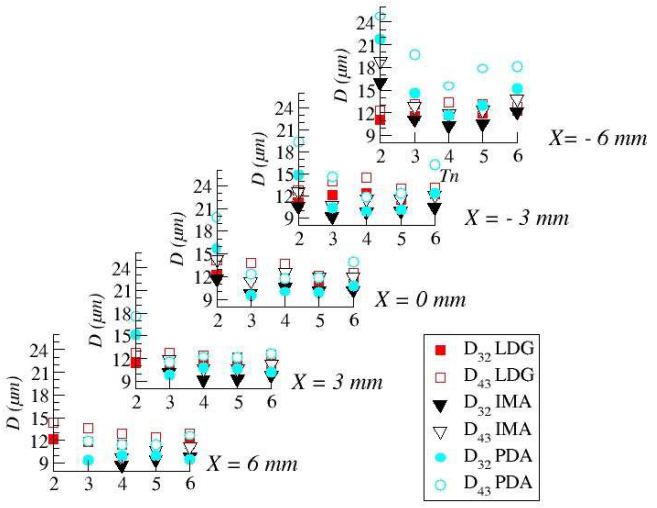

Figure 6: Comparison of the mean diameters versus Time periods T_n @ z=30mm

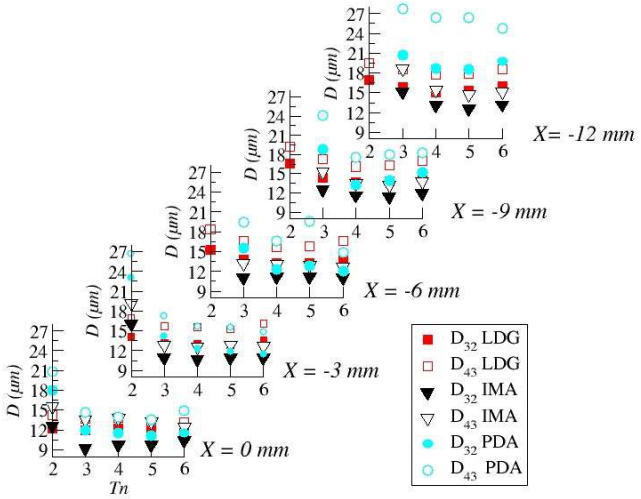

Figure 7: Comparison of the mean diameters versus Time periods T_n @ z=60mm

Figure 7 shows the comparison of the mean diameters for the downstream position z = 60 mm for $x \leq 0$ mm. The trends are the same and the values are in a good agreement in the dense zone of the spray. Here again, IMA gives lower values than PDA and LDG, and PDA gives the highest ones, particularly for the extreme position (x=- 12 mm).

3.2 Probability density function (pdf)

Spatial-averaged volume-weighted drop size distributions are compared in figure 8 for z= 30mm and in figure 9 for z= 60mm, both for time periods T3 and T4. Distributions all present a peak around D = 10 µm but differences on the left edge of the distributions (D< 4 µm) can be noticed. LDG distributions start at 6 µm whereas the minimum diameter for the two other techniques is of the order of 2 µm. However, after computation of the drop size distributions, droplets of diameter smaller than 2 µm were observed. Whereas LDG is supposed to detect particle sizes from 1.9 µm to 200 µm, the computation allows to extend the minimum diameter of the distribution down to 0.5 µm. The detector cannot physically detect these small droplets and the measurement of such small drops is not reliable. Moreover, the drop size distributions of LDG were post-treated to suppress a noisy signal (in the scattering diagrams) for the range $90 < D < 130$ µm. This noise was due to the beam steering effect induced by droplet evaporation in V_m^{LDG} that creates a thermal gradient around the droplets. The resulting signal perturbs randomly the scattering diagram. Fortunately, this noise is completely decorrelated from the main signal.

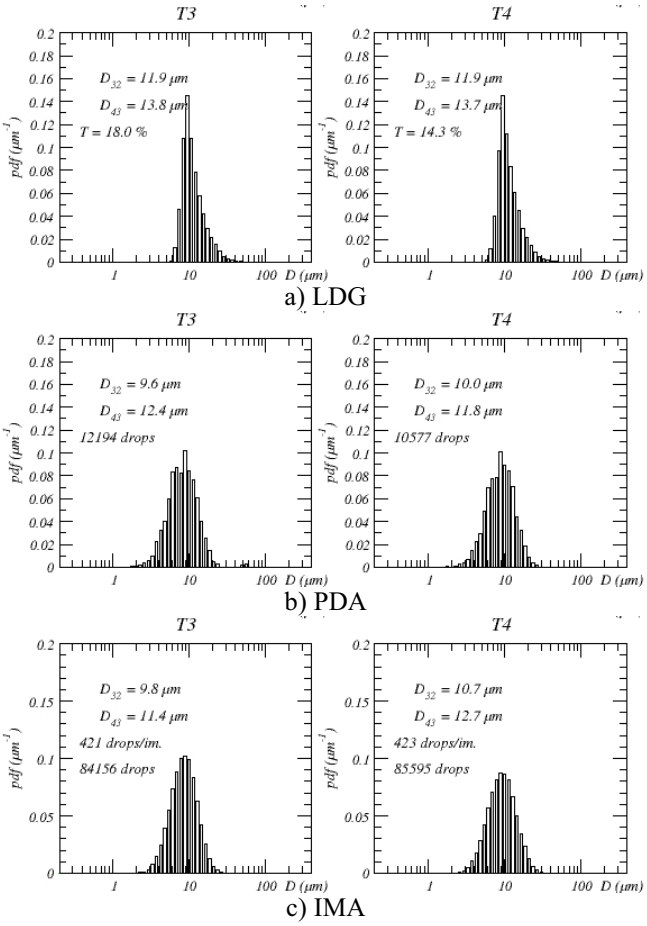

Figure 8: Comparison of drop size distributions @ z = 30 mm, for the time periods T_3 and T_4

It must be noted that distributions given by LDG are smoothed, even if not forced to fit a given law, whereas those for PDA and IMA are not. However, PDA and IMA produce smooth distributions as soon as a sufficient number of drops is counted. It can be seen also on figures 8 and 9 that IMA distributions are not truncated for the smallest diameters, indicating that the image resolution is well suited for the diameter range of the spray. IMA even gives the smallest mean diameters, compared to PDA and LDG. This is induced by the effective depth of filed of IMA as discussed above.

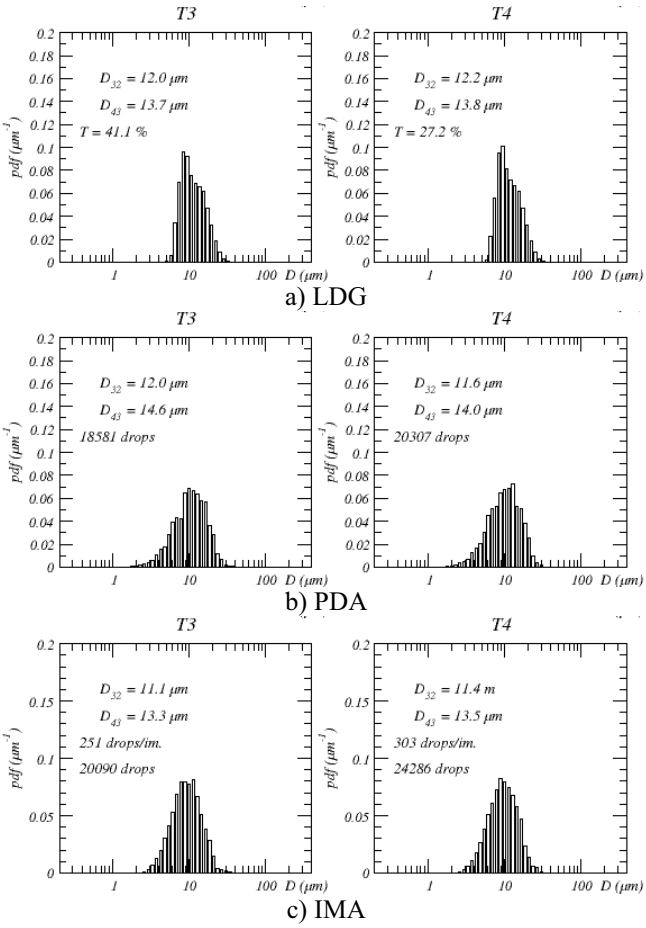

Figure 9: Comparison of drop size distributions @ z = 60 mm, for the time periods T_3 and T_4

3.3 Velocity measurements (PDA)

The velocity measurements presented in figure 10 for the downstream position z = 30 mm and during the steady phase of the flow (time periods T_3 and T_4) show a little correlation between the axial velocity and the droplet diameter for droplet diameters in the range $15 < D < 30$ µm. For $3 < D < 15$ µm, the velocity is almost independent of the drop size and equal to 55-60 m/s. Droplets bigger than 15 µm have more inertia and are less sensitive to the aerodynamic forces. Thus, the velocity increases with diameter from 60 to around 85 m/s. For the smallest drops ($D < 3$ µm), there is no particular rule because very few droplets are detected by PDA and the reliability of measurements on such small drops is arguable.

Temporally, a decrease of the axial velocity has been observed from the beginning to the end of the injection. This can be understood by the fact that the first droplets going out from the nozzle are rapidly slowed down by the ambient air. These drops are quickly evaporating and it remains big droplets that have much more inertia and thus speed. The following droplets are protected by the head of the spray and evaporate less rapidly. Those drops are smaller, have less inertia, and thus are moving slower.

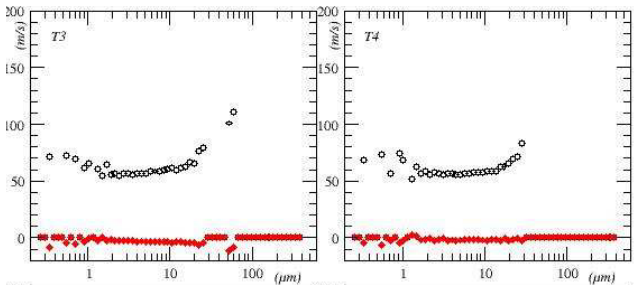

Figure 10: Mean droplet axial (empty symbols) and radial (filled symbols) velocities measured by PDA @ z=30mm and x=0mm

As for the mean diameters, velocities are different for each side of the jet 3, as we can see on figure 11. Velocities are higher on the side of the jet where it is interacting with the other jets ($x > 0$). For $x = 6$ mm (see figure 11 a) , velocities are roughly constant: axial velocity is about 20 m/s and radial velocity 3 m/s for time T5. For time T6, axial velocity is lower: about 10 m/s and radial velocity is 3 m/s. It means that the majority of the droplets are ejected from the jet and dragged away by the other jets.

On the other side ($x \leq 0$ mm), both axial and radial components of the velocity are lower, where the jet is facing the ambient air. For $x = -6$ mm (see figure 11 c), the radial velocity is positive for diameters $D < 5$ µm, indicating that the smallest droplets are moving back to the jet (corroborating the presence of a recirculation zone). For $D > 30$ µm, the radial velocity reaches a minimum of -5 m/s and the axial velocity is maximum (-30 m/s), indicating a ballistic behaviour of the largest drops.

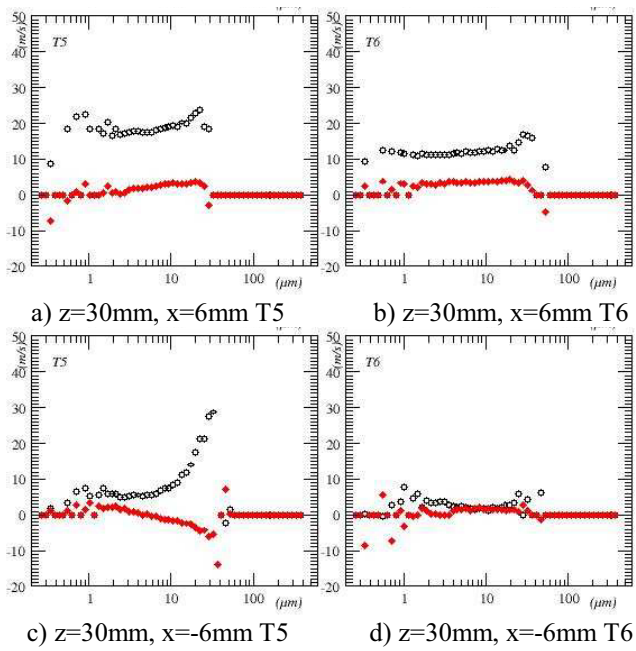

Figure 11: Mean droplet axial (empty symbols) and radial (filled symbols) velocities measured by PDA @ z=30mm on the edges of the spray

Negative axial velocities detected on the very edge of the spray, as we can see on figure 12, confirm the presence of recirculation zones. For the downstream position z = 60 mm, the axial velocity of small droplets ($D < 10$ µm) is negative and equal to ≈ -3 m/s. The smallest droplets are thus moving

back, carried by the ambient air. The presence of negative axial velocity has been observed only on the side of the jet facing the air, i.e. x < 0.

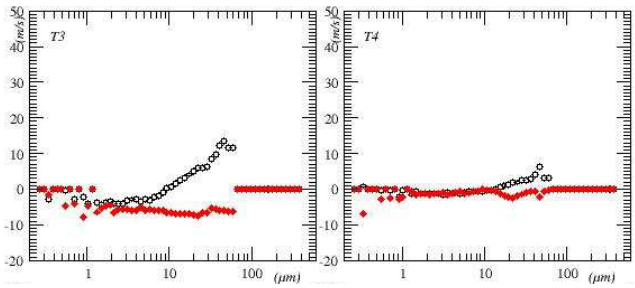

Figure 12: Mean droplet axial (empty symbols) and radial (filled symbols) velocities measured by PDA @ z=60mm and x=-12mm

3.4 Droplet morphology

The advantage of IMA technique is its ability to characterize the droplet morphology. Four shape parameters have been defined by Blaisot et al.[4] in order to characterize objects of various shapes: the Sphericity *Sp*, the Ellipticity ε, the Irregularity φ, and the Uniformity η. Our image processing have been calibrated with synthetic images of objects such as spheres, ellipses and Cassini ovals. These objects have been chosen because they reproduce well the shape of drops and their shape parameters can be obtained analytically. A spherical object corresponds to the quadruplet (ε, S_p, φ, η) = (1, 0, 1, 0).

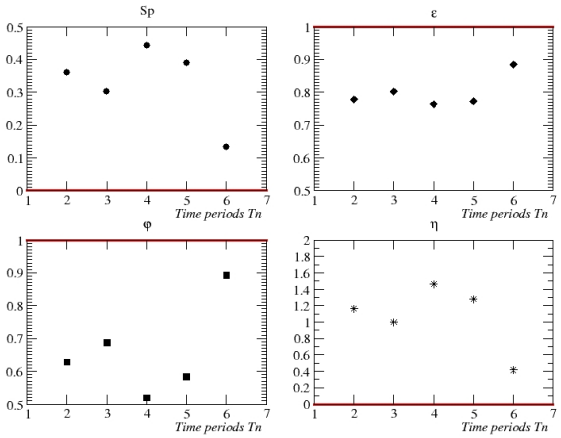

Figure 13: Mean droplet shape parameters (Sp, ε, φ, η) measured by IMA @ z=30mm, x=0

A shape parameter quadruplet is associated to each drop. Figure 13 presents the evolution of the mean value of those parameters for the position z =30 mm, x =0. The morphology is evolving toward the spherical shape during the injection, as ε and φ tend towards 1 and η and S_p tend towards 0.

The shape of the droplets is thus evolving during the time periods T3 to T6 whereas the mean diameters are roughly constant for these time periods (see Figure 6). This means that even when the drop size is stable, the droplet morphology can still evolve.

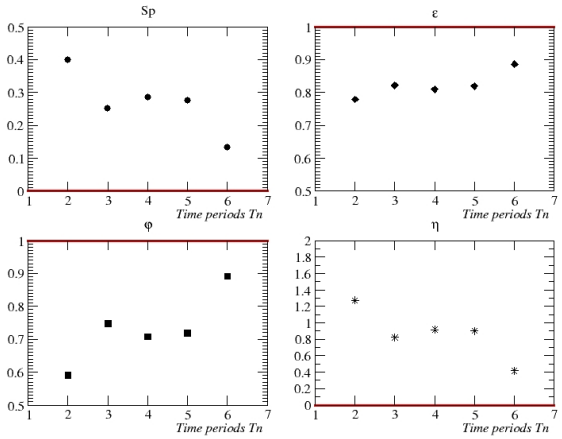

Figure 14: Mean droplet shape parameters (Sp, ε, φ, η) measured by IMA @ z=60mm, x=0

The same behaviour is found for the position z=60 mm, x=0 (see figure 14). Until the time period T3, the droplets are far from the spherical shape. Then the drop shape seems to reach a plateau during the stationary period. For the last time period T6, the droplets are close to the spherical shape.

4. CONCLUSION

This work shows that measurements done by three different drop-sizing techniques (PDA, IMG and LDG) can be compared satisfactorily when applied to a gasoline spray produced by a high-pressure injector. Basic principles of the three techniques are quite different so coherent measurements can be obtained only with a minimum post-processing of the data. One of the main difficulties encountered was due to the non-stationary flow. Indeed, the comparison of the techniques can only be correct if similar samples of the spray drops are considered. Thereby, the difference in detection volumes induces a bias. A correction of this bias was obtained by delaying the time period of PDA sampling relatively to the time period of LDG and IMA. The drop-size distributions of PDA and IMA were also converted to volume-weighted distributions to be comparable to those given by LDG. Moreover, the time-averaged measurements of the PDA were converted to spatial-averaged, thanks to the velocity data given by this technique.

The three techniques are in a rather good agreement on the global shape of the drop size distributions. Furthermore, even if the drop size distributions present some discrepancies, the mean diameters D_{32} and D_{43} are quite similar and above all, the trends are the same for the spatial or the temporal variations. Using these mean diameters is thus appropriated to initialize or calibrate a CFD code for the spray. Indeed, the measurement of these mean diameters seems to be very reliable in this case.

The three techniques show that the mean diameters globally decrease along the injection duration. The mean diameters are also found to increase on the leading edge and on the side of the jet, where the drops are directly facing surrounding air, so where the conditions are favourable to a fast evaporation of the smallest droplets.

It is easy to perform LDG measurements. Moreover LDG provides also a size distribution which can be useful to run an industrial code initialized with a given size distribution law (Rosin-Ramler in most cases). LDG gives a good overall vision of the spray and provides a reliable measure if the spray is dense enough. But it suffers from a lack of spatial

resolution. This could be an advantage when the complete size distribution of a spray not too wide is wanted. In case of a thin jet, the measurement point on the edge of the spray can be perturbed by the presence of other jet on the optical path of the laser beam.

The PDA measurements can take a long time and require numerous injections for distribution to be statistically robust. Indeed, low concentration regions of the spray lead to a very low measurement data rate. To construct a statistically representative drop size distribution, a minimum of 10 000 drops is necessary. This number of drops is all the more hard to reach when temporal analysis is performed. The number of drops listed for each time period is not only different for each period but cannot be imposed at the beginning of the experiment. At least 200 000 drops where demanded for each measurement point with PDA but this was sometimes not sufficient to obtained the necessary number of drops, especially for the first time periods (T1 and T2).

The larger lateral dimensions of the measurement volume of IMA compared to those of PDA are favourable to reduce the experiment time needed to obtain the desired number of drops to construct the distributions. However, the frame rate (~10 image/sec) prevents from time-resolved measurements to be performed with this technique. Thus, as for PDA, a high number of injections must be done in order to obtain statistically robust distributions. IMA measurements tend to give slightly lower values for D_{32} and D_{43}. However, the difference with the other techniques is not so marked and can be due to the effective depth of filed of IMA that is smaller than the length of the other measurement volumes.

Information concerning the morphology of the drops shows that even if the drop size is stable, the droplet morphology can still evolve. Moreover, for the first time periods T1 and T2, the mean droplet shape is not spherical. This can induce a bias in the measurement of the diameters by PDA and LDG.

The time-resolved measurements presented in this paper show that the temporal variation of the diameters is significant. Thus the characterization of the spray must include the time analysis. This time analysis is easier and more rapid to perform with LDG. The advantage of PDA is of course its ability to measure drop velocities. In this case, it shows different trajectories of the droplets on each side of the spray. This can represent a key parameter for the design of a combustion chamber for example. However, PDA measurements demand very precise settings of the optics and technical and practical ability to perform reliable measurements. An alternative choice to LDG and PDA could be IMA. Moreover, this technique can be enhanced when coupled with a particle tracking method to give velocity measurements. This coupling will be tested in a future work.

NOMENCLATURE

Symbol	Quantity	SI Unit
D	Drop diameter	µm
D_{32}	Sauter mean diameter	µm
D_{43}	Mean diameter of the volume-weighted distribution	µm
Δ	Span factor	dimensionless
D_{max}	Maximum Diameter measured with PDA	µm
n	Refractive index	dimensionless
A	Attenuation of light (LDG)	dimensionless
T	Transmission of light (LDG)	dimensionless
U,V	Axial and radial velocities	m/s
x,y,z	Coordinates relative to the nozzle outlet	mm
Vm	Measurement Volume	mm^3
ϕ	Off-axis angle of the receiver of PDA	deg
λ	Wave length	nm
f	Focal length	mm
PSF	Point Spread Function (IMA)	µm
f_v	Size distribution by volume	1/µm
f_n	Size distribution by number	dimensionless
Sp	Sphericity	dimensionless
ε	Ellipticity	dimensionless
φ	Irregularity	dimensionless
η	Uniformity	dimensionless
γ	Lateral Magnification	dimensionless

REFERENCES

[1] K. Triballier, J. Cousin and C. Dumouchel , A technical Study on the Spraytec performances: influence of multiple light scattering and multi-modal drop-size distribution measurements, *Experiments in Fluids,* vol. 35, pp. 347-356, 2003.

[2] G. Gréhan, G. Gouesbet, A. Naqwi, and F. Durst, Particle Trajectory Effects in Phase Doppler Systems: Computations and Experiments, *Part. Part. Syst. Charact*, vol. 10, pp. 332-338, 1993.

[3] G. Gréhan, G. Gouesbet, A. Naqwi, and F. Durst, Trajectory Ambiguities in Phase Doppler Systems: Study of a Near-Forward and a Near-Backward Geometry, *Part. Part. Syst. Charact*, vol. 11, pp. 133-144, 1994.

[4] J.B. Blaisot and J.Yon, Droplet size and morphology characterization for dense sprays by image processing: application to the Diesel spray, *Experiments in Fluids*, vol. 39, pp. 977-994, 2005.

[5] Corcoran T. E., Hitron R., Humphrey W., Chigier N., Optical Measurement of Nebulizer Sprays: A Quantitative Comparison of Diffraction, Phase Doppler Interferometry, and Time of Flight Techniques, *J. Aerosols Sci.*, vol. 31, n°1, pp. 35-50, 2000.

[6] Lee G. Dodge, Deborah J. Rhodes and Rolf D. Reitz, Drop-size measurement techniques for sprays: comparison of Malvern laser-diffraction and Aerometrics phase/Doppler, *Applied Optics*, vol.26, n° 11, pp. 2144-2154, 1987.